Pharmacological Characterization of the Serotonin-sensitive Potassium Channel of *Aplysia* Sensory Neurons

MICHAEL J. SHUSTER and STEVEN A. SIEGELBAUM

From the Center for Neurobiology and Behavior, Department of Pharmacology, and Howard Hughes Medical Institute, Columbia University, New York 10032

ABSTRACT The effects of a variety of K^+ channel blockers on current flow through single serotonin-sensitive K^+ channels (the S channels) of *Aplysia* sensory neurons were studied using the patch-clamp technique. Tetraethylammonium (TEA), 4-aminopyridine (4-AP), and Co^{2+} and Ba^{2+} were first applied to the external membrane surface using cell-free outside-out patches. At concentrations up to 10 mM, these agents had little or no effect on single S-channel currents. At higher concentrations, external TEA acted as a fast open-channel blocker, reducing the single-channel current amplitude according to a simple one-to-one binding scheme with an apparent K_d of 90 mM. Blockade by external TEA is voltage independent. Internal TEA also acts as an open-channel blocker, with an apparent K_d of ~40 mM and a relatively weak voltage dependence, corresponding to an apparent electrical distance to the internal TEA-binding site of 0.1. Both internal and external TEA block the open channel selectively, with an affinity that is 10–100-fold greater than the affinity for the closed channel. Internal Ba^{2+} acts as a slow channel blocker, producing long closures of the channel, and binding with an apparent K_d of ~25–30 μM. These results show that single S-channel currents share a similar pharmacological profile with the macroscopic S current previously characterized with voltage clamp. On the basis of these results, a structural model for S-channel opening is proposed.

INTRODUCTION

Molluscan neuronal cell bodies contain a number of time- and voltage-dependent K^+ currents, including a delayed rectifier current ($I_{K,V}$), an early transient current (I_A), and a Ca^{2+}-activated current ($I_{K,Ca}$) (see D. J. Adams et al., 1980, for review). In addition, *Aplysia* sensory neurons contain a serotonin-sensitive K^+ current (the S current) that contributes to the resting K^+ conductance and to the repolarization of the action potential in these cells (Klein and Kandel, 1980; Klein et al., 1982). Serotonin reduces the magnitude of the S current by a cAMP-dependent

Address reprint requests to Dr. Steven A. Siegelbaum, Dept. of Pharmacology, College of Physicians and Surgeons of Columbia University, 630 W. 168th St., New York, NY 10032. Dr. Shuster's present address is Dept. of Biochemistry and Biophysics, University of California at San Francisco, San Francisco, CA 94143.

J. GEN. PHYSIOL. © The Rockefeller University Press · 0022-1295/87/10/0587/22$2.00

Volume 90 October 1987 587–608

mechanism that results in a slow depolarization of the sensory neuron resting potential, an increase in the action potential duration, and an increase in transmitter release from the sensory neuron presynaptic terminals (Klein and Kandel, 1978; Kandel and Schwartz, 1982).

Voltage-clamp studies show that the S current can be distinguished from the other molluscan K^+ currents by several criteria (Klein et al., 1982; Pollock et al., 1985). The S current is active at both resting and depolarized potentials, does not inactivate with maintained depolarization, shows an outwardly rectifying current-voltage relation, and is modulated by serotonin. The S current also displays a distinctive pharmacological profile in that it is not blocked by 50–100 mM tetraethylammonium (TEA), concentrations that largely inhibit $I_{K,V}$ (Meech and Standen, 1975; Thompson, 1977; Hermann and Gorman, 1981) and $I_{K,Ca}$ (Meech and Standen, 1975; Hermann and Gorman, 1981; but cf. Thompson, 1977). Nor is the S current blocked by 10 mM Ba^{2+}, which also inhibits $I_{K,V}$ and $I_{K,Ca}$ (Gorman and Hermann, 1979; D. J. Adams and Gage, 1980). Similar results have been obtained for an S current in *Helix* neurons (Paupardin-Tritsch et al., 1981).

Using single-channel recording, we previously identified a serotonin-sensitive K^+ channel (the S channel) in *Aplysia* sensory neurons that shares many of the features of the macroscopic S current (Siegelbaum et al., 1982; Camardo et al., 1983). The S channel, like the macroscopic S current, is active at both the resting potential and at depolarized potentials, does not inactivate, shows an outwardly rectifying steady state current-voltage curve, and is closed in an all-or-none manner by serotonin via a cAMP-dependent phosphorylation reaction (Shuster et al., 1985).

Do the S channels also have a pharmacological profile similar to that of the macroscopic S current? Here we report results of experiments that study the effects of a number of K^+-channel blockers on single S-channel currents in cell-free inside-out and outside-out membrane patches. Our results show that the pharmacological properties of single S-channel currents are similar to those of the macroscopic S current. In addition, these experiments allow us to compare the pharmacological profile of the S channels with that of other known K^+ channels. Finally, our results provide indirect information about conformational changes in the S-channel protein associated with channel opening. Some of these results have appeared in an abstract (Shuster and Siegelbaum, 1986).

METHODS

Preparation

Abdominal ganglia from *Aplysia californica* were pinned ventral side up in a recording chamber lined with Sylgard (Dow Corning Corp., Midland, MI), and the sensory cell cluster was exposed by desheathing the left hemiganglion. For some experiments, the desheathed ganglion was exposed to trypsin (0.1–0.2%, type IX, Sigma Chemical Co., St. Louis, MO) for 10–15 min at room temperature (20–25°C) to digest connective tissue and remove glia. This facilitated seal formation between the patch electrode and the sensory cell membrane but made the sensory neurons more fragile. No differences were noted in channel properties between enzyme-treated and untreated neurons.

Patch-Clamp Recordings

Single K^+ channels were recorded from sensory neurons using standard techniques (Hamill et al., 1981). Electrodes were pulled from borosilicate glass micropipettes (Rochester Scientific Co., Rochester, NY) and were fire-polished under a compound microscope using a Pt/Ir filament coated with a bead of borosilicate glass. For some experiments, the electrode shank was coated with Sylgard 184 silicone-elastic polymer to reduce electrode capacitance. Electrode resistances were between 0.5 and 2 MΩ. For most experiments in which inside-out cell-free patches were used, electrodes were filled with a normal artificial seawater solution (see below).

A L/M-EPC5 (List-Medical, Darmstadt, Federal Republic of Germany) patch-clamp amplifier was used to record channel currents. Currents were filtered at 1 kHz using an eight-pole low-pass Bessel filter (model 902LPF, Frequency Devices, Inc., Haverhill, MA) and were stored on magnetic tape using an FM tape recorder (model 3964A, Hewlett-Packard Co., Palo Alto, CA). Currents were analyzed later using an LSI 11–23 laboratory computer (Digital Equipment Corp., Marlboro, MA). For some experiments, single-channel currents were played back from tape at a reduced speed onto a Brush chart recorder (Gould, Inc., Cleveland, OH) and analyzed by hand. The details of the analysis are described along with the individual experiments.

Solutions and Drugs

The artificial seawater contained (millimolar): 460 NaCl, 55 $MgCl_2$, 11 $CaCl_2$, 10 KCl, 10 Tris buffer, pH 7.6. In most experiments with inside-out patches, the electrode was filled with artificial seawater and the bath contained an intracellular-like high-K^+, low-Ca^{2+} solution composed of (millimolar): 10 NaCl, 2 $MgCl_2$, 1 $CaCl_2$, 360 KCl, 20 K-HEPES, 1.5 EGTA, 272 sucrose, pH 7.4 (internal medium). The free Ca^{2+} in this solution was estimated to be 100 nM using the EGTA affinity constants in Bjerrum et al. (1957). For recordings with outside-out patches, electrodes were filled with the high-K^+ intracellular medium. Drugs were bath applied. TEA-Cl was obtained from Eastman Kodak Co., Rochester, NY, and 4-AP, serotonin creatinine sulfate, and apamin were obtained from Sigma Chemical Co. In experiments with internal Ba^{2+}, $BaCl_2$ was added to the above internal solution. Free Ba^{2+} concentrations were calculated using the H^+, Ca^{2+}, Mg^{2+}, and Ba^{2+} affinity constants of EGTA from Bjerrum et al. (1957) and a correction for ionic strength (Martell and Smith, 1974).

RESULTS

The S Channel and Macroscopic S Current Have Similar Pharmacological Profiles

Our first goal in these experiments was to determine whether any common K^+-channel blockers alter current flow through single S channels when applied to the external surface of the membrane. External application of 10 mM TEA (Fig. 1*A*), 5 mM 4-AP (Fig. 1*B*), 10 mM Ba^{2+}, or 10 mM Co^{2+} had no marked effect on single S-channel currents. However, 10 mM TEA produced a small (10–15%), consistent reduction in the apparent single-channel current amplitude. These results were confirmed in three or four separate experiments for each agent (Table I). In two experiments, we also found that the bee venom apamin, a selective blocker of a voltage-independent Ca^{2+}-activated K^+ current (Hugues et al., 1982; Pennefather et al., 1985), had no effect on single S-channel currents.

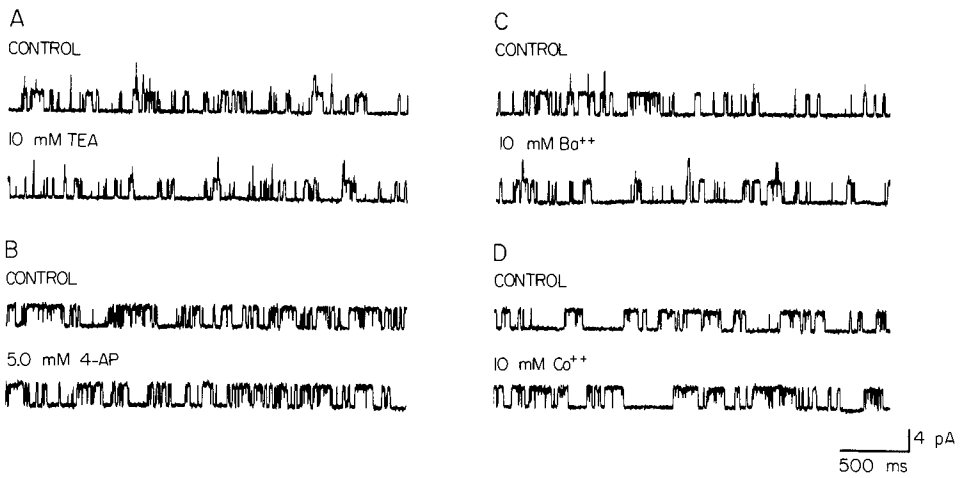

FIGURE 1. The S channel is insensitive to K^+-channel blockers. Single-channel records from outside-out patches showing channel currents before (control) and after addition of blocking agents to the bath (external solution). In all traces, the membrane potential was held at 0 mV. *A* and *C* are from one patch; *B* and *D* are from another patch. The bath solution contained normal ASW; the pipette contained internal medium. Divalent cations were substituted for Ca^{2+}. Currents were filtered at 1 kHz.

The relative insensitivity of the single S-channel currents to external TEA and Ba^{2+} is in agreement with previous studies on the macroscopic S current (Klein et al., 1982; Pollock et al., 1985). The only major discrepancy with the macroscopic results lies in the effects of externally applied Co^{2+}. While external Co^{2+} had no effect on single S-channel currents (Fig. 1 *D*), it did reduce the magnitude of the macroscopic S current, although the extent of this inhibition was somewhat variable (Paupardin-Tritsch et al., 1981; Klein et al., 1982). The inhibitory action of Co^{2+} on the macroscopic S current is puzzling since the S current is neither a

TABLE I

Pharmacological Profile of S Channels in Outside-Out Membrane Patches

Drug	Concentration	*n*	Effect
4-AP	5 mM	1	None
	10 mM	2	None
Ba^{2+}	10 mM	4	None
Co^{2+}	10 mM	5	None
Apamin	10 nM	1	None
	10 μM	1	None
5-HT	100 μM	3	None
TEA	>10 mM	6	Decreased *i*

Ca^{2+} current nor a Ca^{2+}-dependent K^+ current, the currents most susceptible to blockade by Co^{2+}. Two possible explanations for the effects of Co^{2+} on the macroscopic S current are that Co^{2+} interferes with the modulation of the channel by serotonin (e.g., by binding to the receptor or inhibiting adenylate cyclase) or that Co^{2+} directly blocks the S channel (Paupardin-Tritsch et al., 1981; Klein et al., 1982). Our single-channel results are consistent with the former explanation.

Using outside-out patches, we also studied the action of external serotonin on single S-channel currents. Under these conditions, application of 100 μM serotonin to outside-out patches produced no change in channel activity ($n = 3$; data not shown). Since the "intracellular" solution in the patch pipette contained no ATP (or any other nucleotide) to support metabolic reactions, these experiments confirm that the modulation of the S channel by serotonin is mediated by a second messenger. In addition, serotonin does not lead to the activation of any other channel currents in the outside-out patches. These results are summarized in Table I.

External and Internal TEA Reduce the S-Channel Current Amplitude

We have studied the effects of both external and internal TEA over a wide concentration range, both to provide insight into the channel's TEA-binding sites and because unpublished results suggest that even 400 mM TEA has little effect on the macroscopic S current (Klein, M., and B. Hochner, personal communication; Pollock, J. D., personal communication).

Fig. 2 shows that external TEA produced a dose-dependent reduction in the apparent single S-channel current amplitude in outside-out patches. With higher concentrations of TEA, there was also an increase in the apparent probability of a channel being open. This increase in open probability was especially evident with 300 mM TEA, where the current record spends much less time at the zero level (corresponding to no open channels) than it does in the absence of TEA.

These effects of TEA on S-channel currents were consistently observed in all experiments using outside-out patches ($n = 6$). The onset and recovery from blockade upon switching to and from TEA-containing solutions reached an equilibrium within a few seconds, essentially at a rate limited by the speed of our perfusion system. Fig. 2*B* shows a steady state dose-response curve for the reduction in channel current amplitude as a function of the TEA concentration, using data pooled from the six experiments with outside-out patches. The data are plotted in terms of the fractional reduction of the apparent single-channel current amplitude, F_i, defined as 1 − (current amplitude in TEA)/(control current amplitude). The data are well fitted by a simple one-to-one binding reaction, assuming that the fractional reduction in the single-channel current amplitude is equal to the occupancy of the TEA-binding site:

$$F_i = \frac{[\text{TEA}]}{(K_d + [\text{TEA}])}, \quad (1)$$

where K_d is the apparent dissociation constant. Eq. 1 was fitted to the data by a nonlinear least-squares routine (solid curve), yielding an estimate of 88.5 mM for K_d.

In contrast to the delayed rectifier channel of squid axon, where internal TEA is a much more potent blocker than external TEA (Tasaki and Hagiwara, 1957), the S channel shows about the same sensitivity to internal and external TEA.

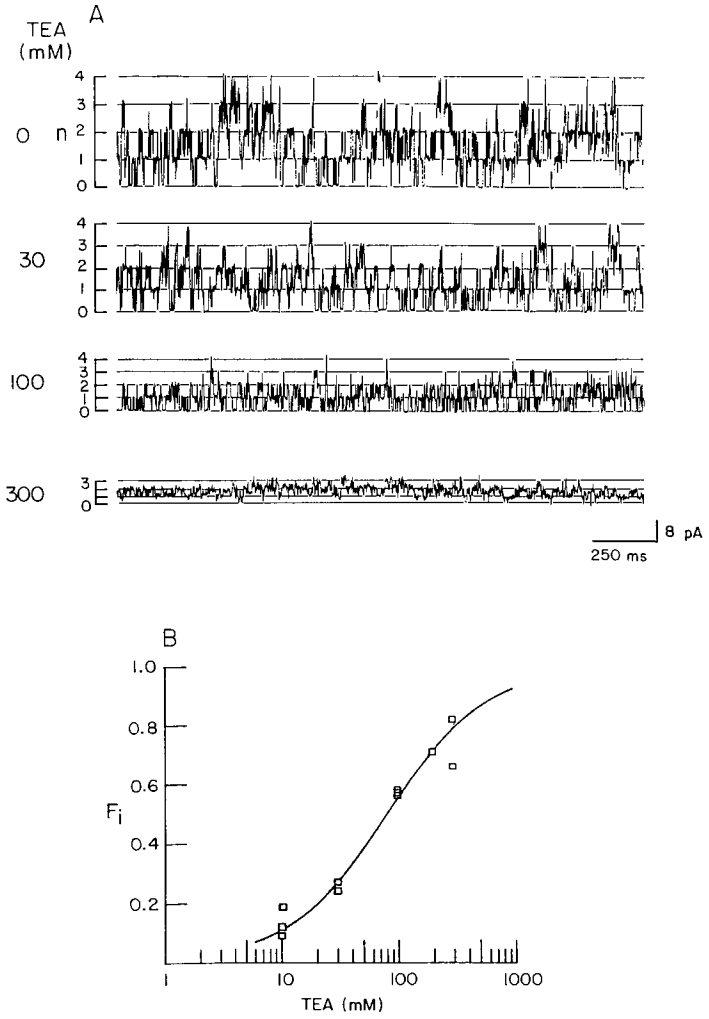

FIGURE 2. Effects of external TEA on S-channel currents. (*A*) Single-channel current records in presence of increasing concentrations of TEA (concentrations are indicated on the left). The ordinate (n) shows the number of channels open. Records were obtained from an outside-out patch at +60 mV (absolute membrane potential). The patch pipette contained internal medium; the bath contained normal ASW. TEA replaced external Na^+ on an equimolar basis. Current records were filtered at 1 kHz. (*B*) Dose-response curve for reduction in the single-channel unit current amplitude. Data are plotted in terms of F_i, the fractional reduction in i (see text). The data here have been pooled from six separate experiments on different outside-out membrane patches at 0 mV patch potential. The smooth curve is a nonlinear least-squares fit of Eq. 1 to the data. Each symbol represents a separate measure of F_i.

Fig. 3*A* shows that internal TEA produced a dose-dependent reduction in the apparent single-channel current amplitude. The dose-response curve for the fractional reduction in the channel current amplitude (F_i) as a function of TEA concentration is plotted in Fig. 3*B*. The data, pooled from three experiments, are well fitted by the simple one-to-one binding scheme of Eq. 1, with an apparent

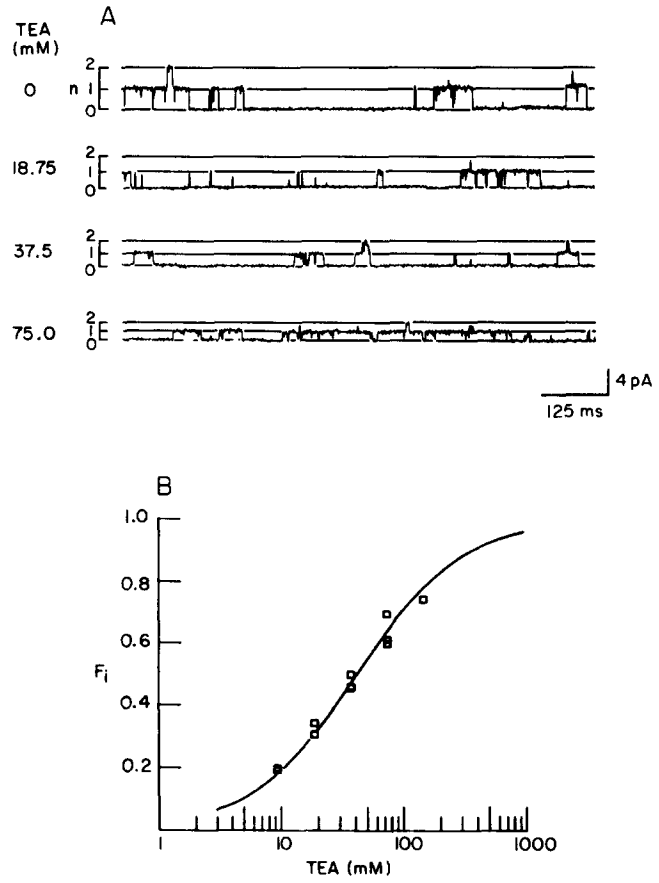

FIGURE 3. Effects of internal TEA on S-channel currents. (*A*) Single-channel records from an inside-out patch in response to series of internal TEA concentrations (applied to the bath). The membrane potential was held at 0 mV. There was ASW in the pipette and intracellular medium in the bath. Records were filtered at 1 kHz. TEA was substituted for sucrose on an equiosmotic basis. (*B*) Dose-response curve for reduction in the apparent single-channel amplitude by internal TEA. Data were pooled from three separate experiments. The curve shows a fit of Eq. 1 to the data. In all experiments, $V_m = 0$ mV. Each square represents a separate determination.

K_d of 42 mM. Thus, the affinity of the channel for internal TEA is similar but not identical to its affinity for external TEA.

In one sense, these results agree with the macroscopic voltage-clamp data since rather high concentrations of extracellular TEA were required to block current

flow through the S channel. However, there is an apparent quantitative discrepancy since the voltage-clamp data indicate that, at least under some conditions, the macroscopic S current is not significantly inhibited by up to 400 mM TEA, a concentration that reduces the single S-channel current amplitude to <20% of its control value.

One possible explanation for this apparent discrepancy is that the steady state macroscopic S current reflects the mean single S-channel current, $\langle I \rangle$, given by the product Npi (where N is the number of functional channels in the membrane and p is the probability that a given channel is open), and not just the single-channel current amplitude as measured above. Fig. 4 plots the effects of TEA on the mean single S-channel current in two outside-out patches. Estimates of

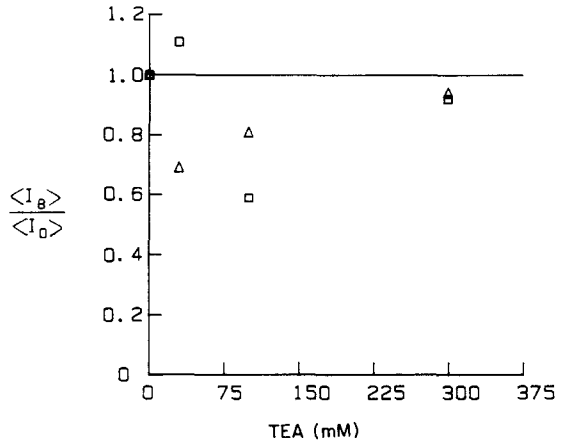

FIGURE 4. Effect of external TEA on the mean single S-channel current, $\langle I \rangle$. Data were obtained from two experiments (different symbols) using outside-out patches. The mean single-channel currents at each TEA concentration were obtained by integrating the single-channel current record for 10–30 s and then dividing by the total time period. The mean current in the presence of TEA ($\langle I_B \rangle$) is normalized by the mean current in the absence of TEA ($\langle I_0 \rangle$) and plotted as a function of drug concentration. The membrane potential was 0 mV; there was internal medium in the pipette and normal ASW in the bath. The initial open probabilities in these two experiments were 0.05 (□) and 0.1 (△).

$\langle I \rangle$ were obtained by integrating 10–30-s stretches of single-channel current records at different concentrations of TEA. It is clear that external TEA had relatively little effect on the mean S-channel current, despite its consistent action to reduce the single-channel current amplitude. For example, while 300 mM TEA caused a three- to fourfold decrease in i, the mean channel current was reduced by <20%. In other experiments, high concentrations of TEA produced a somewhat greater reduction in $\langle I \rangle$, although the effects on the mean channel current were always smaller than the observed reduction in the single-channel current amplitude. A possible reason for this variability is discussed below.

The discrepancy between the magnitude of the effects of TEA on the mean current and the single-channel current amplitude results from a second action

of TEA to increase the apparent probability that a channel is in the open state (Fig. 5). Increasing concentrations of either extracellular (*A*) or intracellular (*B*) TEA produce a dose-dependent increase in the apparent open probability that counteracts the decrease in the single-channel current amplitude with TEA. We found no consistent effect of TEA on N, the number of active channels in a

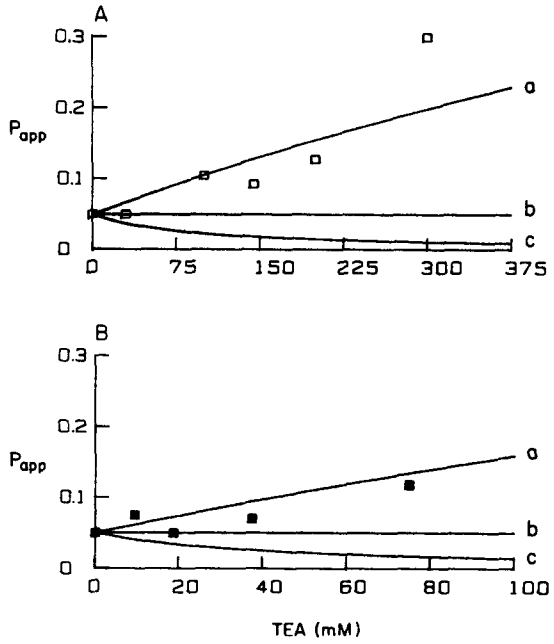

FIGURE 5. TEA increases the apparent channel open probability. For each concentration of TEA, N and p were estimated from fits of the binomial distribution (e.g., Patlak and Horn, 1982). The ordinate plots the apparent channel open probability. (*A*) Data from an outside-out patch, showing effects of external TEA. Curve *a* shows the predictions of the pure open-channel block model (Eq. 5); curve *b* shows predictions for a nonselective blocker ($K_{dO} = K_{dC}$; Eq. 8), and curve *c* shows the predictions for selective closed-channel blocker ($K_{dO} \gg K_{dC}$; Eq. 8). Curve *a* was drawn using measured value for p_o (initial open probability in the absence of TEA) of 0.05 and for K_d of 80.6 mM, obtained from the dose-dependent reduction by TEA of the unit current amplitude. In this patch, n = 3 (from binomial analysis). (*B*) Similar data showing an increase in the apparent open probability in inside-out patch in response to internal TEA. Curves are drawn as in *A* using measured values for p_o of 0.05 and for K_d of 38.5 mM. In this patch, $n = 1$.

patch. In summary, TEA is a very weak blocker of the mean single S-channel current, in good agreement with the voltage-clamp results.

Open-Channel Block Scheme for TEA

The opposing effects of TEA on i and p can be explained by the simple sequential

open-channel block model (Armstrong, 1975; P. R. Adams, 1976; Neher and Steinbach, 1978):

$$C \longleftrightarrow O + B \underset{k_b}{\overset{k_f}{\rightleftharpoons}} OB, \tag{2}$$

where C is the channel in the closed state, O is the channel in the open state, B is the channel-blocker molecule, OB is a nonconducting open-blocked channel, k_f is the first-order forward rate constant for channel block, and k_b is the rate of unblocking. We assume that the blocker alters neither the normal single-channel current amplitude nor the normal open-closed gating reaction.

For certain channel blockers, the kinetics of the blocking and unblocking transitions are slow enough (on a millisecond time scale) that the individual blockings and unblockings can be observed. At the single-channel level, these agents transform the normal rectangular current pulses associated with channel opening into a burst of rapid openings and closings caused by blockings and unblockings of the open channel (Neher and Steinbach, 1978).

In contrast, other blockers have much more rapid kinetics (on the order of microseconds), similar to the time scale of ion permeation (Yellen, 1984*a*). For these fast blockers, the individual current pulses associated with the blockings and unblockings cannot be resolved, because of the limited bandwidth of typical recordings (<10 kHz). Thus, the rapid burst of openings appears as only a single opening with a reduced amplitude owing to the low-pass filtering. We show below that this model accounts for all of the effects of TEA reported above.

The apparent channel current amplitude in the presence of a fast blocker, i_B, is equal to the true open-channel current amplitude, i_o, scaled by the fraction of time that a channel spends in the open state as it cycles between states O and OB: [O]/([O] + [OB]). With increasing concentrations of blocker, there is a dose-dependent reduction in the apparent single-channel current amplitude as the equilibrium of the reaction between the open and open-blocked channel is shifted toward the open-blocked state. The fractional reduction in the single-channel amplitude, F_i (i.e., $1 - i_B/i_o$), plotted in Figs. 2 and 3, it thus given by the fraction of time that the channel spends in the open-blocked state during an apparent opening:

$$F_i = \frac{[OB]}{[OB] + [O]} = \frac{[B]}{[K_d] + [B]}. \tag{3}$$

Eq. 3 is identical to the one-to-one binding scheme of Eq. 1.

The open-channel block model also accounts for the relative insensitivity of the mean S-channel current to concentrations of TEA that significantly reduce the apparent single-channel current amplitude. In the absence of TEA, the mean channel current, $\langle I_0 \rangle$, is given by the product Nip_o, where p_o is the open probability in the absence of drug: [O]/([O] + [C]). The mean current in the presence of TEA, $\langle I_B \rangle$, is given by the product Nip_B, where p_B is the probability that the channel is in state O in the presence of TEA: [O]/([O] + [C] + [OB]). According to the open-channel block scheme of Eq. 2, this is given by:

$$p_B = \frac{p_o K_d}{K_d + p_o[B]}. \quad (4)$$

Since TEA only alters channel open probability, the ratio $\langle I_B \rangle / \langle I_0 \rangle$ (plotted in Fig. 4) equals the ratio p_B/p_o:

$$\frac{\langle I_B \rangle}{\langle I_0 \rangle} = \frac{K_d}{K_d + p_o[B]}. \quad (5)$$

According to Eq. 5, the effectiveness of a given concentration of blocker in reducing $\langle I \rangle$ is scaled down by a factor equal to the initial channel open probability, p_o. In the two experiments shown in Fig. 4, p_o was 0.05 and 0.1, which explains the small effect of even 300 mM TEA (roughly $4K_d$) on $\langle I \rangle$. In other experiments, where p_o was higher, TEA caused a larger reduction in $\langle I \rangle$, as predicted by Eq. 5.

The open-channel block model is also in quantitative agreement with the increase in the apparent open probability (p_{app}) with TEA. Since we cannot resolve the brief blockings or openings in TEA, p_{app} is given by the probability that the channel is in the compound state (O or OB):

$$p_{app} = \frac{[O] + [OB]}{[C] + [O] + [OB]} = \frac{p_o(1 + B/K_d)}{1 + p_o(B/K_d)}. \quad (6)$$

The curves labeled *a* in Fig. 5 are plotted using Eq. 6. No free parameters are required since p_o is measured directly from the single-channel current record in the absence of TEA and K_d is determined independently from the observed reduction in unit current amplitude (e.g., from Figs. 2*B* and 3*B*). The data for both external (Fig. 5*A*) and internal (Fig. 5*B*) TEA are reasonably well described by Eq. 6, within the scatter of the experimental data. A similar agreement with the open-channel block model was observed in two other experiments with external TEA and one other experiment with internal TEA.

In contrast, the data are not consistent with blocking schemes where TEA acts either as a nonselective blocker, binding to open and closed channels with equal affinity (curve *b*), or as a pure closed-channel blocker (curve *c*). These curves are based on a general cyclic model for channel block (see P. R. Adams, 1977):

$$\begin{array}{ccc} C & \longleftrightarrow & O \\ {\scriptstyle K_{dC}}\uparrow\downarrow & & \uparrow\downarrow{\scriptstyle K_{dO}} \\ CB & \longleftrightarrow & OB \end{array} \quad (7)$$

According to the cyclic model, a blocking drug binds to a single site on the channel with different affinities depending on whether the channel is closed (K_{dC}) or open (K_{dO}). Unlike the pure open-channel block model, this scheme allows for a significant reduction in $\langle I \rangle$, regardless of p_o, owing to the interaction of drug with the closed channel. The effect on p_{app} of a blocking drug following this general reaction scheme depends on the relative affinities of the closed and open channels for blocker:

$$p_{app} = \frac{p_o(1 + [B]/K_{dO})}{1 + p_o([B]/K_{dO}) + (1 - p_o)([B]/K_{dC})}. \quad (8)$$

Eq. 8 was used to plot curves *a*, *b*, and *c* in Fig. 5 under the limiting conditions where $K_{dC} \gg K_{dO}$, $K_{dC} = K_{dO}$, and $K_{dC} \gg K_{dO}$, respectively. Exploring intermediate values for K_{dC}/K_{dO} shows that the data are most consistent with models where the open channel binds both external and internal TEA selectively with an affinity that is 10–100-fold greater than the affinity of the closed channel for TEA. Unfortunately, the scatter in the experimental points prevents a more accurate determination of the relative affinities of the closed and open channels for TEA.

Voltage Dependence of Current Blockade with TEA

The similarity between the actions of internal and external TEA raises the question as to whether the binding sites for internal and external TEA are distinct or whether there is but a single site within the channel that is accessible to TEA applied to either side of the membrane. We have investigated the voltage dependence of TEA action as an approach to answering this question. Since TEA is a monovalent cation, drug binding should be influenced by membrane potential if the binding site (or sites) lies within the membrane's electric field. For blockade by external TEA, the dissociation constant will depend on voltage according to:

$$K_d(V) = K_d(0)\exp(dFV/RT), \quad (9)$$

(e.g., see Woodhull, 1973). Here $K_d(0)$ is the dissociation constant measured at 0 mV, V is membrane potential, d is the fraction of the membrane field "sensed" by TEA at the binding site, and R, T, and F have their usual meanings. A similar expression applies to block by internal TEA, except that the argument of the exponential term is now negative. If internal and external TEA bind to a common site within the channel, the sum of their electrical distances should be close to 1 (in the limit of large voltage displacements opposing TEA entry).

To determine the extent to which drug action was influenced by membrane potential, single-channel current-voltage relations were measured in the absence and presence of TEA. Fig. 6*A* illustrates this approach for an outside-out patch exposed to a series of different TEA concentrations. In the absence of TEA (squares), the single-channel current-voltage relation displays a characteristic outward rectification. With increasing concentrations of TEA, there is a progressive reduction in the single-channel current amplitude over the entire voltage range. The extent to which the single-channel current amplitude is reduced by a given concentration of TEA at the various membrane potentials is roughly comparable.

To obtain a more quantitative measure of voltage dependence, apparent dissociation constants for TEA binding were obtained at each membrane potential by fitting Eq. 1 to the observed reduction in the single-channel amplitude. The open symbols in Fig. 6*B* plot, on a semilogarithmic scale, the values of K_d determined in this manner as a function of membrane potential for blockade

with external TEA. There is virtually no voltage dependence to the block produced by external TEA, as the slope of the plot is not significantly different from zero (i.e., $d = 0$). Thus, the external TEA-binding site appears to be located at the external edge of the membrane, near the outside mouth of the channel.

An identical procedure was used to assess the voltage dependence of channel blockade with internal TEA. The triangles in Fig. 6*B* show the effect of membrane potential on the effective dissociation constant for internal TEA. At this side of the membrane, TEA shows a greater voltage dependence, although it is still relatively weak. A +257-mV change in potential decreases K_d e-fold, yielding an estimate for d of ~0.1. Thus, the internal TEA-binding site is relatively close to the inside edge of the electric field. Since the sum of the electrical distances with internal and external TEA is $\ll 1$, it is unlikely that external and internal TEA bind to a common site within the channel (see also Yellen, 1984*a*).

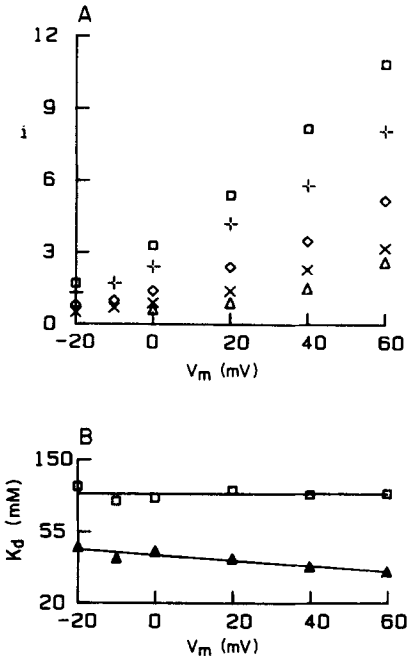

FIGURE 6. Voltage dependence of current blockade with TEA. (*A*) Single S-channel current-voltage relations in the absence and presence of different concentrations of external TEA. Data were obtained from a single outside-out patch. At each potential, the single-channel current amplitude is an average of 50–100 openings. Concentrations: 0 (□), 30 (+), 100 (◇), 200 (×), and 300 (△) mM TEA. (*B*) Voltage dependence of the apparent K_d values for TEA blockade. Data are plotted on a semilogarithmic scale. The values for K_d at each potential were obtained as described in the text. The squares plot K_d values for blockade by external TEA obtained with outside-out patches. Each symbol is an average K_d from two to five separate experiments. The triangles show average K_d values for blockade by internal TEA obtained from experiments with inside-out patches (for each symbol, $n = 3$). The lines, fitted by linear regression, indicate that the K_d for external TEA shows essentially no voltage dependence (i.e., the slope is not significantly different from zero). The K_d for block by internal TEA decreases e-fold for a 257-mV depolarization.

Raising External K^+ Alters the Voltage Dependence of Block by Internal TEA

More direct evidence that TEA blocks current flow by binding to a site within the channel pore comes from studies of the influence of the extracellular K^+ concentration on the blockade produced by internal TEA. The weak voltage-

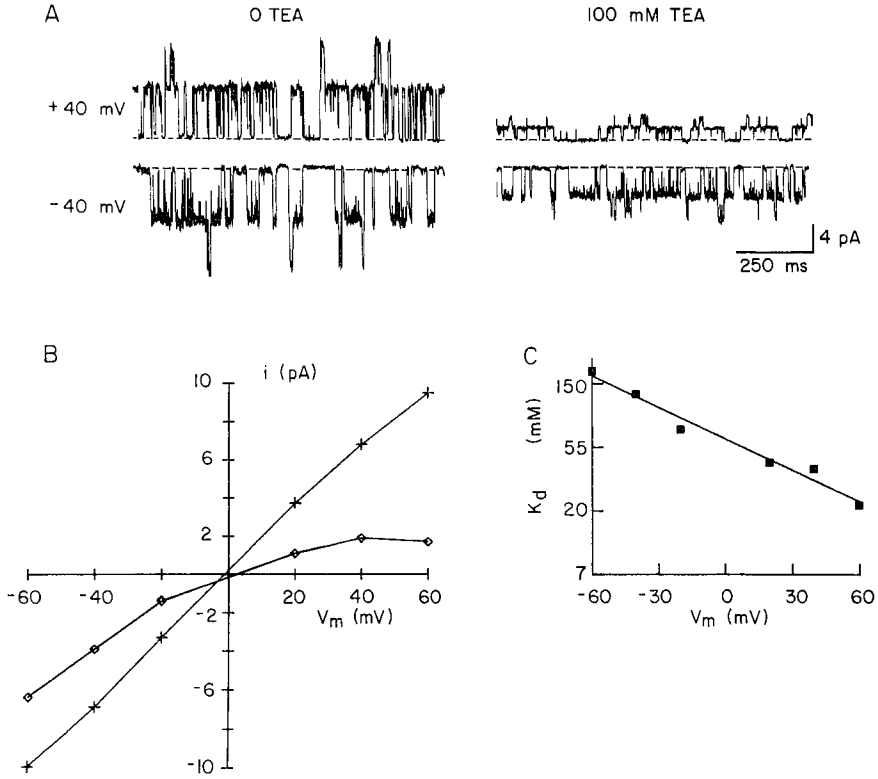

FIGURE 7. External K^+ alters the voltage dependence of blockade with internal TEA. (*A*) Effects of TEA on single-channel currents from an inside-out patch. Channel currents are shown in absence and presence of 100 mM TEA at two membrane potentials. Both bath and pipette solutions contained internal medium (360 mM KCl, 10 mM NaCl). The dashed line shows the zero-current level (no channels open). Records were filtered at 1 kHz. TEA-Cl was substituted for sucrose on an equiosmotic basis. (*B*) Single-channel current-voltage relation in the absence (+) or presence (◇) of 100 mM TEA. TEA induced a marked rectification in the current-voltage curve. The small apparent change in reversal potential with TEA is not significant. (*C*) Dependence of K_d on membrane potential. K_d was measured over a wide voltage range and is plotted as function of V_m on a semilogarithmic scale. The line was fitted by linear regression, with a slope that indicates an e-fold decrease in K_d for a 62-mV depolarization. At 0 mV, K_d = 63 mM.

dependent action of internal TEA was observed above with inside-out patches under conditions where there was an intracellular-like solution in the bath (360 mM KCl, 10 mM NaCl) and a normal Na^+ seawater solution in the pipette (460 mM NaCl, 10 mM KCl). Fig. 7 shows that raising the external KCl concentration

markedly increased the voltage dependence of the blockade produced by internal TEA. Fig. 7*A* compares S-channel current records at −40 and at +40 mV, before and after addition of 100 mM TEA to the internal solution. At the more negative voltage, the apparent single-channel current amplitude was reduced by TEA to 50% of its initial value. Upon depolarizing the patch potential to +40 mV, there was a twofold increase in the extent of blockade with TEA and the channel current amplitude was reduced to 25% of its initial value.

The voltage-dependent action of 100 mM TEA in high external K^+ is illustrated over a wider potential range in Fig. 7*B*. Like its action in squid giant axon (Armstrong and Binstock, 1965), internal TEA induced a marked rectification in the current-voltage curve, with comparatively greater inhibition seen at more positive potentials. A similar result was obtained with 50 mM internal TEA. At each membrane potential, effective K_d values were determined (from Eq. 1) and these are plotted as a function of voltage on a semilogarithmic scale in Fig. 7*C*. There is a significant increase in the slope of the plot compared with the data obtained for the blockade by internal TEA with low extracellular K^+ (Fig. 6*B*). With high external K^+ (Fig. 7*C*), K_d decreased e-fold for a +62-mV change in voltage, yielding an effective electrical distance of 0.4 (compared with 0.1 measured in Fig. 6*B*). Raising external K^+ also increased the apparent K_d (measured at 0 mV) for internal TEA from ~40 mM (10 mM external K^+) to 60 mM (360 mM external K^+).

The simplest explanation for the effect of external K^+ is that TEA enters and binds to a site within the channel pore, where it interacts with K ions. This interaction might be due to either a knock-off reaction, where K^+ actually repels TEA (e.g., Armstrong, 1975; Yellen, 1984*b*), or a simple competition for a binding site within the channel (e.g., Vergara and Latorre, 1983). We have not yet determined whether block by external TEA also is influenced by the internal K^+ concentration.

Internal Ba^{2+} Produces a Slow Blockade of S-Channel Currents

The similarity between the action of internal and external TEA suggests that the two mouths of the S channel may be structurally similar. To test this idea further, we compared the effects of other K^+-channel blockers when applied to either the internal and external surfaces of the membrane. While we found that 4-AP (10 mM) had no effect on channel activity at either surface of the membrane, Ba^{2+} selectively blocked S-channel currents when applied to the inside of the membrane.

Fig. 8 shows the effects of Ba^{2+} applied to an inside-out patch with two active S channels that displayed an initial high probability of opening ($p = 0.76$). The time base is compressed to emphasize events that occurred on a slow time scale. In the absence of Ba^{2+}, the channels were open for a large fraction of the time with occasional closures lasting several seconds (which on this time scale appear as gaps in the current record). Addition of micromolar Ba^{2+} to the bath greatly increased the number of long-lasting closures, reducing both the mean S-channel current as well as the probability that the S channel was open. In the presence of 52 μM Ba^{2+}, the channel open probability was reduced from its initial value

of 0.76 to 0.32. We detected no change in the single-channel current amplitude with up to 3 mM Ba^{2+}. As the concentration of internal Ba^{2+} increased, the frequency of long closings increased and there was a dose-dependent reduction in both the mean S-channel current and the probability that a channel was open. The dose-response curve for the reduction in open probability with Ba^{2+} can be reasonably well fitted by the simple open-channel block model (Eq. 6) with a K_d of 20 μM at 0 mV, although we have not yet determined whether, in fact, Ba^{2+} is selective for the open state of the channel.

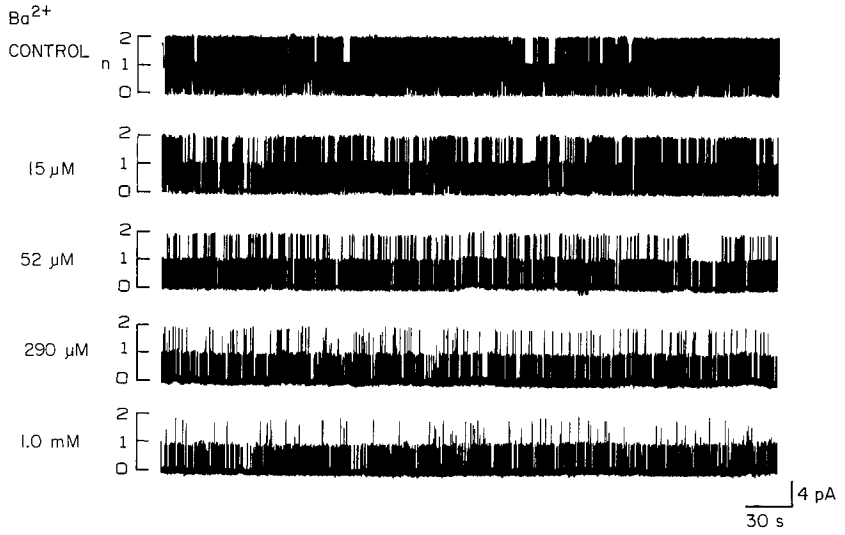

FIGURE 8. Effect of internal Ba^{2+} on single S-channel currents. Single-channel current records are from an inside-out patch with two active channels. The records are displayed on a compressed time base to emphasize slow events. The ordinate (n) indicates the number of open channels. The top trace shows a control record of channel current activity in the absence of Ba^{2+}. Both channels are open during most of the record. Occasional long closures lasting 1–5 s (gaps at $n = 2$) appear in the absence of Ba^{2+}. The lower traces show channel currents in presence of increasing concentrations of internal Ba^{2+}. The free Ba^{2+} concentration was calculated using EGTA stability constants for Ba^{2+}, Ca^{2+}, and Mg^{2+} from Bjerrum et al. (1987). The total $BaCl_2$ added to normal internal medium solution was (top to bottom) 0, 0.1875, 0.375, 0.75, and 1.5 mM. The calculated free Ba^{2+} concentrations are indicated on the left. The measured channel open probabilities were 0.76, 0.5, 0.3, 0.13, and 0.04 in the presence of 0, 15, 52, and 290 μM and 1.0 mM Ba^{2+}, respectively. The membrane potential was 0 mV. There was ASW in the pipette and intracellular medium in the bath. Records were filtered at 1 kHz.

DISCUSSION

These experiments provide a pharmacological profile for the S channel that is summarized in Table I. We found that the S channel has certain basic pharmacological properties in common with other K^+ channels. It is blocked by TEA at both the external and internal sides of the membrane and by Ba^{2+} at the internal

membrane surface. However, the S channel can be distinguished from most other K^+ channels by its insensitivity to blockade by external Ba^{2+} (10 mM) or 4-AP (10 mM). These experiments also provide a means for identifying the orientation of S channels reconstituted in lipid bilayers since Ba^{2+} blocks only from the internal side of the membrane.

The single-channel results are in reasonably good agreement with previous voltage-clamp experiments that characterized the macroscopic S current, I_S (Klein and Kandel, 1980; Klein et al., 1982; Pollock et al., 1985). This supports the view that the S channel identified in patch-clamp studies (Siegelbaum et al., 1982) plays a major role in generating the macroscopic I_S. However, these results do not rule out the possibility that other currents owing to channels distinct from the S channel also contribute to the macroscopic serotonin response (e.g., Baxter and Byrne, 1986).

Comparison of Microscopic and Macroscopic TEA Actions

The relatively low affinity of TEA for the S channel is in qualitative agreement with the weak blocking effects of external TEA on the macroscopic S current. Results from four separate studies indicate that 30–100 mM TEA does not completely inhibit the macroscopic serotonin response (Klein and Kandel, 1978; Paupardin-Tritsch et al., 1981; Pollock et al., 1985; Baxter and Byrne, 1986). However, a complete dose-response curve for blockade of the macroscopic S current with TEA has not yet been published. Unpublished results of M. Klein and B. Hochner suggest that 400 mM TEA produces a <50% reduction in the S current. In contrast, D. A. Baxter and J. H. Byrne (personal communication) found that the response to serotonin is reduced by half with 50 mM TEA in the external solution.

Our single-channel results show that the K_d for the binding of external TEA to the open channel is ~90 mM, in rough agreement with the value reported by Baxter and Byrne for block of the macroscopic S current. However, according to the open-channel block model, the efficacy of TEA in blocking the macroscopic current depends on the initial probability that the S channel is open (see Eq. 5).

The discrepancy among the different findings on the TEA sensitivity of the macroscopic S current could be explained if, under different conditions in different preparations, there were some variability in the initial S-channel open probability. In previous experiments, we reported such a variability in single S-channel gating properties and found that S channels undergo apparently spontaneous switches in gating modes from a low probability state ($p < 0.1$) to a much higher probability state ($p > 0.5$) (Siegelbaum et al., 1982). Recent experiments with the peptide Phe-Met-Arg-Pheamide (FMRFamide) show that S-channel gating is under control by this inhibitory modulatory transmitter (Belardetti et al., 1987; Brezina et al., 1987). Acting through a second messenger distinct from cAMP, FMRFamide opens S channels by causing an increase in the channel open probability (Belardetti et al., 1987). A variability in the extent to which this inhibitory second-messenger system is activated under resting conditions could account for the observed differences in the TEA sensitivity of the macroscopic S current.

Implications of the Open-Channel Block Model

These experiments also provide some insight into the nature of the conformational change that is associated with the transition from the closed to the open state of the S channel. Our results show that the channel has two TEA-binding sites with similar affinities, located near the external and internal mouths of the channel (Fig. 9). At both sites, the affinity of the drug for the open channel is at least 10–100 times higher than it is for the closed channel. While previous studies have reported interactions of drug binding and channel gating at either the internal or external membrane surfaces, our results provide evidence for selective open-channel block at both sides of the membrane.

This result implies that the conformational change that underlies S-channel opening must result in changes in channel structure near both the internal and external TEA-binding sites. Thus, S-channel opening probably involves a wide-

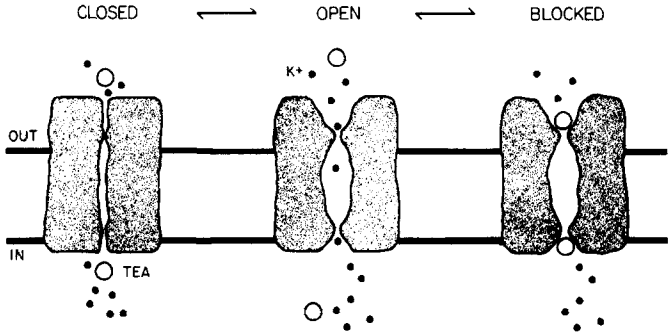

FIGURE 9. Structural model for S-channel opening. The channel is shown in three states in presence of TEA: closed, open, and open-blocked. Internal and external TEA preferentially bind to sites near the two mouths of the channel when the channel is open. This suggests that as the channel opens, there is a simultaneous conformational change at both the external and internal binding sites, illustrated here as a general widening of the channel pore.

spread change in the conformation of the channel macromolecule that spans the length of the membrane, rather than a highly localized structural change expected for the rotation of a discrete "gate" (Fig. 9). Similar mechanisms for channel opening have recently been proposed by Unwin and Ennis (1984) for the gap junction channel on the basis of structural data, and by Zimmerberg and Parsegian (1986) for the mitochondrial channel porin on the basis of effects of hydrostatic pressure on channel gating.

Comparison of the Blocking Actions of TEA and Ba^{2+} on Different K^+ channels

How do the actions of TEA and Ba^{2+} on the S channel reported here compare with previous studies on two other well-characterized K^+ channels, the delayed rectifier K^+ channel and the Ca^{2+}-activated K^+ channel? Table II summarizes these results by comparing values of K_d for blockade and apparent electrical distances to the binding sites within the channels. With all three channels, internal TEA acts as an open-channel blocker, although there is a considerable variability

in the sensitivity to TEA among the different channels. The Ca^{2+}-activated K^+ channel of bovine chromaffin cells (Yellen, 1984*a*) and the S channel show very similar K_d values for blockade by internal TEA and identical electrical distances. The S channel and the Ca^{2+}-activated K^+ channel are also similar in that TEA acts for both channels as a very rapid channel blocker, causing a dose-dependent reduction in the apparent single-channel amplitude.

There is considerably less similarity among the external TEA receptors of these three channels. The delayed rectifier in squid giant axon is completely insensitive to externally applied TEA (Tasaki and Hagiwara, 1957; Armstrong and Binstock, 1965). However, both the delayed rectifier in frog node (Hille,

TABLE II

Comparison of TEA and Ba^{2+} Action on Different K^+ Channels

		TEA			Ba^{2+}		
Channel	Site	K_d	d	Reference	K_d	d	Reference
		mM					
$I_{K,V}$ (squid axon)	External	200		Tasaki and Hagiwara (1957)	150 mM	0.75	Armstrong et al. (1982)
	Internal	1.0	0.2	French and Shoukimas (1981)	0.1 μM	0.5	Eaton and Brodwick (1980)
						1.0	Armstrong et al. (1982)
$I_{K,V}$ (frog node)	External	0.4	0	Hille (1967)			
	Internal	5.0	0.2	Hille (1975)			
$I_{K,V}$ (molluscan)	External	6.0	+	Hermann and Gorman (1981)			
		8.0	−	Thompson (1977)			
$I_{K,Ca}$ (molluscan)	External	0.4	+	Hermann and Gorman (1981)			
		>100	−	Thompson (1977)			
$I_{K,Ca}$ (mammalian)	External	0.2	0.2	Yellen (1984*a*)	1.8 mM	0.35	Vergara and Latorre (1983)
		0.3		Blatz and Magleby (1984)			
	Internal	27	0.1	Yellen (1984*a*)	36 μM	0.8	Vergara and Latorre (1983)
		60	0.26	Blatz and Magleby (1984)			
S channel (*Aplysia*)	External	90	0		≫10 mM		
	Internal	40	0.1		28 μM		

Values shown are the apparent dissociation constants (K_d) for drug action measured at 0 mV and the apparent electrical distance to the drug-binding site within the channel (d). Drugs were applied to the external and internal membrane surfaces. Where no measurable voltage dependence was found, $d = 0$. The plus sign indicates experiments where d was not measured, but where there was a clear voltage-dependent drug action.

1967) and the Ca^{2+}-activated K^+ channel (Wong et al., 1982; Blatz and Magleby, 1984; Yellen, 1984*a*) are very sensitive to external TEA. The S channel appears to be an intermediate case between these extremes. While the blockade by external TEA is voltage independent for both the S channel and the delayed rectifier channel in the node of Ranvier, the blockade of the Ca^{2+}-activated K^+ channel is measurably voltage dependent.

A comparison of the blocking actions of the various K^+ channels by Ba^{2+} also suggests that the internal channel-blocking sites are more similar to each other than the external sites. The delayed rectifier of squid giant axon is the most

sensitive to internal Ba^{2+}, with a K_d at 0 mV of 0.1 μM (Eaton and Brodwick, 1980). The Ca^{2+}-activated K^+ channel (Vergara and Latorre, 1983) and the S channel are two orders of magnitude less sensitive to blockade and show very similar K_d values for internal Ba^{2+}. The blockade by internal Ba^{2+} of both the delayed rectifier channel and the Ca^{2+}-activated K^+ channel is markedly voltage dependent. We have not yet determined the degree to which voltage influences the blockade of the S channel with internal Ba^{2+}.

The S channel and the Ca^{2+}-activated K^+ channel are thus similar in their sensitivities to blockade by both internal TEA and internal Ba^{2+}. Under symmetrical KCl conditions, the two channels also show similar single-channel conductances. The single-channel conductance of the S channel, with 360 mM KCl and 10 mM NaCl on either side of the membrane, is ~200 pS (Fig. 7*B*). In symmetrical solutions of 100–200 mM KCl, the Ca^{2+}-activated K^+ channel shows a conductance of ~160–300 pS (Marty, 1983).

The major difference between the S channel and the Ca^{2+}-activated K^+ channel lies in the Ca^{2+} and voltage dependence of their gating reactions. We found that S-channel opening is independent of the internal Ca^{2+} concentration over a range from 10 nM to 1 mM (Camardo et al., 1983; Shuster, M. J., J. S. Camardo, and S. A. Siegelbaum, manuscript in preparation). In addition, the gating of the S channel is generally rather insensitive to membrane potential (Siegelbaum et al., 1982), although the extent of voltage dependence is variable and, under some conditions, a significant voltage dependence can be seen (Siegelbaum et al., 1982; Shuster, M. J., J. S. Camardo, and S. A. Siegelbaum, manuscript in preparation). The similarities we found between the S channel and the Ca^{2+}-activated K^+ channel might indicate that these channels have evolved from a common ancestral K^+ channel or that unrelated K^+ channels have developed similar structural elements to accomplish the common goals of high K^+ selectivity and rapid ion permeation.

We thank Dr. Joe Camardo for help in the early stages of these experiments and Kathrin Hilten for preparing the figures.

M.J.S. is presently a Lucille P. Markey Fellow of the Life Sciences Research Foundation. This work was supported in part by National Institutes of Health grant NS-19569 to S.A.S.

Original version received 26 February 1987 and accepted version received 11 May 1987.

REFERENCES

Adams, D. J., and P. W. Gage. 1980. Divalent ion currents and the delayed potassium conductance in an *Aplysia* neurone. *Journal of Physiology.* 304:297–313.

Adams, D. J., S. Smith, and S. H. Thompson. 1980. Ionic currents in molluscan soma. *Annual Review of Neuroscience.* 3:141–167.

Adams, P. R. 1976. Drug blockade of open end-plate channels. *Journal of Physiology.* 260:531–552.

Adams, P. R. 1977. Voltage jump analysis of procaine action at frog end-plate. *Journal of Physiology.* 268:291–318.

Armstrong, C. M. 1975. K pores of nerve and muscle membrane. *In* Membranes: a Series of Advances. G. Eisenmann, editor. Marcel Dekker, New York. 3:325–358.

Armstrong, C. M., and L. Binstock. 1965. Anomalous rectification in the squid giant axon injected with tetraethylammonium chloride. *Journal of General Physiology.* 48:859–872.

Armstrong, C. M., R. P. Swenson, and S. R. Taylor. 1982. Block of squid axon K channels by internally and externally applied barium ions. *Journal of General Physiology.* 80:663–682.

Baxter, D. A., and J. H. Byrne. 1986. Serotonin-modulated membrane currents in *Aplysia* tail sensory neurons. *Society for Neuroscience Abstracts.* 12:765.

Belardetti, F., E. R. Kandel, and S. A. Siegelbaum. 1987. Neuronal inhibition by the peptide FMRFamide involves opening of S K^+ channels. *Nature.* 325:153–156.

Bjerrum, J., G. Schwarzenbach, and L. G. Sillen. 1957. Stability Constants. Part I: Organic Ligands. The Chemical Society, London.

Blatz, A. L., and K. L. Magleby. 1984. Ion conductance and selectivity of single calcium-activated potassium channels in cultured rat muscle. *Journal of General Physiology.* 84:1–23.

Brezina, V., R. Eckert, and C. Erxleben. 1987. Modulation of potassium conductances by an endogenous neuropeptide in neurones of *Aplysia californica*. *Journal of Physiology.* 382:267–290.

Camardo, J. S., M. J. Shuster, S. A. Siegelbaum, and E. R. Kandel. 1983. Modulation of a specific potassium channel in sensory neurons of *Aplysia* by serotonin and cAMP-dependent protein phosphorylation. *Cold Spring Harbor Symposia on Quantitative Biology.* 48:213–220.

Eaton, D. C., and M. S. Brodwick. 1980. Effect of barium on the potassium conductance of squid axon. *Journal of General Physiology.* 75:727–750.

French, R. J., and J. J. Shoukimas. 1981. Blockage of squid axon conductance by internal tetra-*n*-alkylammonium ions of various sizes. *Biophysical Journal.* 34:271–291.

Gorman, A. L. F., and A. Hermann. 1979. Internal effects of divalent cations on potassium permeability in molluscan neurones. *Journal of Physiology.* 296:393–410.

Hamill, O. P., A. Marty, E. Neher, B. Sakmann, and F. J. Sigworth. 1981. Improved patch-clamp techniques for high-resolution current recording from cells and cell-free membrane patches. *Pflügers Archiv.* 391:85–100.

Hermann, A., and A. L. F. Gorman. 1981. Effects of tetraethylammonium on potassium currents in a molluscan neuron. *Journal of General Physiology.* 78:87–110.

Hille, B. 1967. The selective inhibition of delayed potassium currents in nerve by tetraethylammonium ion. *Journal of General Physiology.* 50:1287–1302.

Hille, B. 1975. Ionic selectivity of Na and K channels of nerve membranes. *In* Membranes: a Series of Advances. G. Eisenman, editor. Marcel Dekker, New York. 3:255–323.

Hugues, M., G. Romey, D. Duval, J.-P. Vincent, and M. Lazdunski. 1982. Apamin as a selective blocker of the calcium-dependent potassium channel in neuroblastoma cells: voltage-clamp and biochemical characterization of the toxin receptor. *Proceedings of the National Academy of Sciences.* 79:1308–1312.

Kandel, E. R., and J. H. Schwartz. 1982. Molecular biology of learning: modulation of transmitter release. *Science.* 218:433–443.

Klein, M., J. Camardo, and E. R. Kandel. 1982. Serotonin modulates a specific potassium current in the sensory neurons that show presynaptic facilitation in *Aplysia*. *Proceedings of the National Academy of Sciences.* 79:5713–5717.

Klein, M., and E. R. Kandel. 1978. Presynaptic modulation of voltage-dependent Ca^{2+} current: mechanism for behavioral sensitization in *Aplysia californica*. *Proceedings of the National Academy of Sciences.* 75:3512–3516.

Klein, M., and E. R. Kandel. 1980. Mechanism of calcium current modulation underlying presynaptic facilitation and behavioral sensitization in *Aplysia*. *Proceedings of the National Academy of Sciences.* 77:6912–6916.

Martell, A. E., and Smith, R. M. 1974. Critical Stability Constants. Plenum Publishing Corp., London.

Marty, A. 1983. Ca^{2+}-dependent K^+ channels with large unitary conductance. *Trends in Neurosciences.* 6:262–265.

Meech, R. W., and N. B. Standen. 1975. Potassium activation in *Helix aspersa* neurones under voltage clamp; a component mediated by calcium influx. *Journal of Physiology.* 249:211–239.

Neher, E., and J. H. Steinbach. 1978. Local anaesthetics transiently block currents through single acetylcholine-receptor channels. *Journal of Physiology.* 277:153–176.

Patlak, J., and R. Horn. 1982. Effect of *N*-bromoacetamide on single sodium channel currents in excised membrane patches. *Journal of General Physiology.* 79:333–351.

Paupardin-Tritsch, D., P. Deterre, and H. M. Gerschenfeld. 1981. Relationship between two voltage-dependent serotonin responses of molluscan neurones. *Brain Research.* 217:201–206.

Pennefather, P., B. Lancaster, P. R. Adams, and R. A. Nicoll. 1985. Two distinct Ca-dependent K currents on bullfrog sympathetic ganglion cells. *Proceedings of the National Academy of Sciences.* 82:3040–3044.

Pollock, J. D., J. S. Camardo, and L. Bernier. 1985. Serotonin and cyclic adenosine 3′:5′-monophosphate modulate the S potassium current in tail sensory neurons in the pleural ganglion of *Aplysia. Journal of Neuroscience.* 7:1862–1871.

Shuster, M. J., J. S. Camardo, S. A. Siegelbaum, and E. R. Kandel. 1985. Cyclic AMP-dependent protein kinase closes the serototonin-sensitive K^+ channels of *Aplysia* sensory neurones in cell-free membrane patches. *Nature.* 313:392–395.

Shuster, M. J., and S. A. Siegelbaum. 1986. Pharmacological characterization of the S potassium channel of *Aplysia* sensory neurons. *Society for Neuroscience Abstracts.* 12:766.

Siegelbaum, S. A., J. S. Camardo, and E. R. Kandel. 1982. Serotonin and cyclic AMP close single K^+ channels in *Aplysia* sensory neurones. *Nature.* 299:413–417.

Tasaki, I., and S. Hagiwara. 1957. Demonstration of two stable potential states in the squid giant axon under tetraethylammonium chloride. *Journal of General Physiology.* 40:859–885.

Thompson, S. H. 1977. Three pharmacologically distinct potassium channels in molluscan neurones. *Journal of Physiology.* 265:465–488.

Unwin, P. N. T., and P. D. Ennis. 1984. Two configurations of a channel-forming membrane protein. *Nature.* 307:609–613.

Vergara, C., and R. Latorre. 1983. Kinetics of Ca^{2+}-activated K^+ channels from rabbit muscle incorporated into planar bilayers. *Journal of General Physiology.* 82:543–568.

Wong, B. S., H. Lecar, and M. Adler. 1982. Single calcium-dependent potassium channels in clonal anterior pituitary cells. *Biophysical Journal.* 39:313–317.

Woodhull, A. M. 1973. Ionic blockage of sodium channels in nerve. *Journal of General Physiology.* 61:687–708.

Yellen, G. 1984*a*. Ionic permeation and blockade in Ca^{2+}-activated K^+ channels of bovine chromaffin cells. *Journal of General Physiology.* 84:157–186.

Yellen, G. 1984*b*. Relief of Na^+ block of Ca^{2+}-activated K^+ channels by external cations. *Journal of General Physiology.* 84:187–199.

Zimmerberg, J., and V. A. Parsegian. 1986. Polymer inaccessible volume changes during opening and closing of a voltage-dependent ionic channel. *Nature.* 323:36–39.